

## LAMINAR FLOW IN A COMPLEX GEOMETRY: A COMPARISON

M. NAPOLITANO

*Istituto di Macchine, Università di Bari, via Re David 200, 70125 Bari, Italy.*

AND

P. ORLANDI

*Dipartimento di Meccanica ed Aeronautica, Università di Roma 'La Sapienza', Roma, Italy*

### SUMMARY

This paper reports on the outcome of a workshop of the IAHR Working Group on Refined Modelling of Flows on the subject of computing laminar flows in complex geometries. Flow inside a channel with a smooth expansion was chosen by the organizers of the workshop as a suitable test case for assessing the capabilities of current numerical methods. The results obtained by fifteen participant groups are presented and compared against a suitable benchmark solution. The most important considerations that emerged at the workshop are briefly reported and the conclusions arising from an analysis and comparison of the various solutions are finally provided.

KEY WORDS Laminar Flows Complex Geometry Numerical Methods

### INTRODUCTION

The continuous and sustained growth in computer speed and memory, as well as the improvements in the accuracy and efficiency of algorithms for solving partial differential equations, have allowed many researchers to attempt to compute flows of practical interest. Most applications involve 'complex geometries', namely domains whose boundaries do not coincide with co-ordinate lines of a Cartesian or any other simple co-ordinate system.

Two methodologies are employed most commonly in computational fluid dynamics (CFD), namely finite differences and finite elements. With regard to the specific task of computing flows in complex geometries, the finite element method appears as the most natural tool, owing to its intrinsic geometric flexibility. However, the finite difference method takes more and more advantage of co-ordinate transformations and grid generation techniques to exploit its superior simplicity and efficiency. Actually, both methodologies have their own merits and deficiencies, so that nothing definite can be said of the superiority of either.

In order to stimulate a fruitful debate among CFD specialists and to assess the capabilities of various numerical methods to deal with laminar flows in complex geometries, the International Association for Hydraulic Research (IAHR) Working Group on Refined Modelling of Flows decided to devote its Fifth Meeting to this specific subject.

The Working Group, aware that more conclusive answers can be drawn from testing different methods on a single well defined problem, also decided to devote a special workshop to the comparison and discussion of the solutions of a test case.

A previous meeting on the numerical treatment of advection<sup>1</sup> had shown that in advection dominated problems the accuracy of numerical schemes is extremely sensitive to the discretization of the advection term. Therefore, a test case was chosen in which the numerical treatment of advection is of a secondary importance, namely the laminar flow through a smooth expansion channel proposed by Roache.<sup>2</sup>

The announcement of the meeting, together with full details of the test case, was sent in advance to a large number of researchers. More than fifteen groups submitted results, which were discussed at the workshop-session of the Fifth IAHR Meeting, held in Rome on 24–25 May 1982 at the Facolta' di Ingegneria dell'Universita' La Sapienza.

The purpose of this paper is to report the outcome of the comparison among the various results and to record the conclusions which emerged from the discussion. It is hoped that this information will prove valuable to the large number of researchers involved in the solution of (laminar) flows in complex geometries.

### TEST PROBLEM

The plane channel flow proposed by Roache<sup>2</sup> was chosen as the test problem for the workshop. The geometry, depicted in Figure 1, depends on the value of the Reynolds number,  $Re$ : the channel becomes longer and straighter as  $Re$  increases and, for  $Re \gg 1$ , a quasi-self-similar solution is obtained.<sup>2</sup>

The lower boundary (solid wall) of the channel is given by the following analytical expression:

$$y_1 = [\tanh(2 - 30x/Re) - \tanh(2)]/2, \tag{1}$$

for  $0 \leq x \leq x_{out} = Re/3$ ; whereas the upper boundary (symmetry plane) is located at  $y_u = 1$ .

The inlet boundary conditions are given in terms of the Cartesian velocity components  $u, v$ , as

$$\left. \begin{aligned} u &= 3(y - y^2/2) \\ v &= 0 \end{aligned} \right\} \text{ for } x = 0, \quad 0 \leq y \leq 1, \tag{2a, b}$$

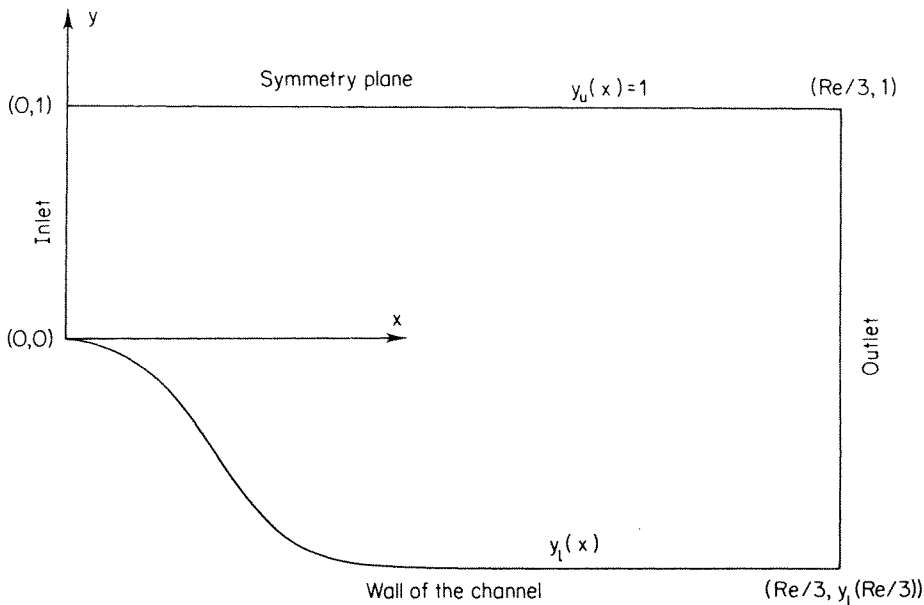


Figure 1. Geometry of the channel for  $Re = 10$

or, for the case of the stream function, as

$$\left. \begin{aligned} \psi &= (3y^2 - y^3)/2 \\ \partial\psi/\partial x &= 0 \end{aligned} \right\} \text{ for } x=0, \quad 0 \leq y \leq 1. \quad (3a, b)$$

The standard no-slip, no-injection conditions are imposed at the wall ( $0 \leq x \leq x_{\text{out}}, y = y_1$ ); symmetry is enforced at  $0 \leq x \leq x_{\text{out}}, y = y_u$ ; the outlet boundary conditions have been left to the choice of each participant.

Two flows were selected as mandatory cases, corresponding to the relatively small values of the Reynolds number  $Re = 10$  and  $Re = 100$ ; the former was chosen because of its rather distorted geometry (see Figure 1) and the latter to assess the dependence of the convergence rate of each method on  $Re$ . Smaller Reynolds numbers were not considered to avoid the major difficulty of providing appropriate inflow and outflow conditions. However, a third optional case characterized by a more significant advection, namely  $Re = 100$  flow inside the  $Re = 10$  channel, was also proposed. A  $21 \times 21$  gridpoints finite difference mesh, or an equivalent finite element discretization, was prescribed in order to allow for a meaningful comparison among the various solutions.

For all flow cases each participant was asked to provide his numerical results in terms of both the vorticity ( $\omega$ ) and the pressure ( $p$ ) distributions along the wall of the channel in order to not privilege the use of the primitive ( $u, v, p$ ) or non-primitive ( $\psi, \omega$ ) variables. The total CPU time required to get a converged solution was also requested, to assess the efficiency of the various numerical methods. The CPU time was made somewhat computer-independent by normalizing it with respect to that required to run a standard Fortran code provided by the organizers of the workshop, P. Orlandi, A. Di Carlo and P. Mele.

## RESULTS AND DISCUSSION

Before comparing the various solutions to the test case, it seems appropriate to report briefly on the principal points which emerged during the workshop.

The major debate among the participant-groups concerned the questionable validity of the inlet boundary conditions, emphasized by the  $Re = 10$  results. Fully developed Poiseuille flow conditions have been prescribed at the inlet, in spite of the non-zero slope of the wall of the channel at  $x = 0$ . As a consequence, there is a singular behaviour at this point,<sup>3</sup> which shows up as a disturbed wall pressure distribution in many of the numerical solutions. Such a singularity has been investigated by Cliffe *et al.*,<sup>3</sup> who also conducted a mesh refinement study to obtain a grid-independent solution. The value of the pressure field in incompressible flows being defined up to an arbitrary additive constant, it was decided to fix the value of the pressure equal to zero on the wall at  $x = x_{\text{out}}/2$ . In this way, the various pressure distribution results are considered to be more meaningful and can be compared more easily. In fact, the usual choice of the inlet or outlet as the reference pressure point could have caused difficulties because of either the presence of the singularity at the inlet or the arbitrariness of the boundary conditions at the outlet.

Some of the participants felt that the problem under investigation was 'too easy' and therefore not suitable to assess the capability of each code to compute flows in complex geometries. Such an opinion, however, cannot be agreed upon *a posteriori*, after the analysis of the various results.

Since a satisfactory analysis and comparison of the results was not completed at the workshop, at its end it was decided that a paper should be written to report and compare the various solutions. The optional flow case having been solved only by a very few groups, it was agreed to devote the paper to the two compulsory cases only. In order to provide the authors of the paper with all of the necessary information, each group was asked to fill in a form requiring the names of the authors and their affiliations, a short summary of the method employed, the main reference describing it in

Table I. Basic information about the contributors

Contributor	Affiliation	Formulation			Computer	Label
		Scheme	Variables			
Alfrink	Delft Hydraulics Laboratory, Netherlands	FD	$u, v, p$	CYBER 175	A	
Cliffe <i>et al.</i>	AERE Harwell, U.K.	FE	$u, v, p$	CRAY 1	CJG	
Demirovic and Gosman	Imperial College London, U.K.	FV	$u, v, p$	CDC 6600	DG	
Goussebaile <i>et al.</i>	Lab. Nat. d'Hydraulique Chatou, France	FD	$u, v, p$	CRAY 1	GBV	
Grandotto	Commissariat a l'Energie Atomique, France	FE	$u, v, p$	CRAY 1	G	
Gujj and Favini	Università di Roma 'La Sapienza', Italy	FD	$u, v, p$	UNIVAC 1100/82	GF	
Huiton	Central Electricity Generating Board, U.K.	FE	$u, v, p$	IBM 3032	H	
Khaletzky	NEYPIC, France	FE	$u, v, p$	AS 7000	K	
Latrobe and Delapierre	Commissariat a l'Energie Atomique, France	FV	$u, v, p$	CDC 7600	LD	
Magi and Napolitano	Università di Bari, Italy	FD	$\psi, \omega$	HP 1000/F	MN	
Porter <i>et al.</i>	AERE Harwell, U.K.	FD	$u, v, p$	IBM 3033	PSW	
Quartapelle and Napolitano	Politecnico di Milano, Italy	FE	$\psi, \omega$	AMDHL 470/V8	QN	
Rastogi	A. S. Veritas Research, Norway	FD	$u, v, p$	UNIVAC 1100	R	
Schonauer	Universität Karlsruhe, West Germany	FD	$\omega, u, v$	SIEMENS 7865	S	
Wada and Adachi	Gen. Res. Inst. of Electric Power Industry, Japan	FD	$\psi, \omega$	CRAY 1	WA1	
Wada and Adachi	Gen. Res. Inst. of Electric Power Industry, Japan	FD	$u, v, p$	CRAY 1	WA2	
		Cartesian				

detail and the computed wall vorticity and pressure at 21 equally spaced  $x/x_{\text{out}}$  locations.

Fifteen groups returned the forms to the organizers. Table I indicates the names of the first author of the group and the affiliations, the numerical formulation and the type of computer and, finally, a label composed by the initials of all the authors, used to identify each group in the Tables summarizing the results. The descriptions and the references for each method, as received from the various contributors, are reported in the Appendix.

Most participants submitted both the pressure and vorticity values for the cases  $Re = 10$  and  $Re = 100$ . The numerical results are given in Tables II–V. For the  $Re = 10$  case the results have also been plotted in Figures 2 and 3 only to provide an immediate rough idea of their behaviour and spreading, and therefore the various curves are not identified. In the absence of an exact reference solution, the grid-independent results obtained by Cliffe *et al.*<sup>3</sup> have been assumed as a benchmark. Such a solution has then been used to compute the average percentage errors  $\varepsilon_\omega$  and  $\varepsilon_p$ , defined according to the following relationships:

$$\varepsilon_\omega = \frac{100}{19} \sum_{i=2}^{20} \left| \frac{\omega_i - \omega_{i\text{CJG}}}{\omega_{i\text{CJG}}} \right|, \quad (4)$$

$$\varepsilon_p = \frac{100}{18} \sum_{i=2}^{20} \left| \frac{p_i - p_{i\text{CJG}}}{p_{i\text{CJG}}} \right|, \quad (5)$$

where  $\omega_i$  and  $p_i$  are the vorticity and pressure at the aforementioned equally spaced points along the wall, computed by each group, and the subscript CJG refers to the benchmark (interpolated) solutions by Cliffe *et al.*<sup>3</sup> It is noteworthy that the values at the gripoints  $x = 0$  and  $x = x_{\text{out}}$  have not been included in the definitions of  $\varepsilon_\omega$  and  $\varepsilon_p$  to reduce the influence of the singularity at the inlet and of the arbitrary outlet boundary conditions. For the case of  $\varepsilon_p$  the (exact) value at  $x = x_{\text{out}}/2$  has also been excluded (see equation (5)). Finally, we would like to point out that  $\varepsilon_\omega$  has been defined so as to account mostly for the region around and inside the separation bubble. This is a rational and appropriate choice and therefore  $\varepsilon_\omega$  is a good quantity to judge the accuracy of the solutions for the present flow cases.

The errors for each method are given in Table VI, which also contains the normalized CPU time and the minimum and outlet vorticity values. From the results in Tables II–VI it clearly appears that:

1. The validity of the solution by Cliffe *et al.*<sup>3</sup> as an adequate benchmark is confirmed by its very good agreement with the results obtained by Schonauer using adaptive, comparably fine,  $46 \times 32$  and  $41 \times 62$  meshes. In Table VI, in fact, Schonauer's results appear as the most accurate ones, being characterized by values of  $\varepsilon_\omega$  as little as 1.74 and 0.44 for the  $Re = 10$  and the  $Re = 100$  flow cases, respectively. The use of two completely different formulations by these two groups, who solve the  $u$ ,  $v$ ,  $p$  equations by finite elements (CJG) and the  $u$ ,  $v$ ,  $\omega$  equations by finite differences (S) provides further evidence of the high accuracy of both solutions.

2. The WA2 solution, using a Cartesian co-ordinate system which requires interpolation to impose the wall boundary conditions, is clearly inadequate to compute the present flows in complex geometries; for the  $Re = 100$  flow case the WA2 solution in Table III is seen to ignore completely the separation phenomenon and has a very large  $\varepsilon_\omega = 135.48$  per cent.

3. In spite of the presumed simplicity of the flows to be computed, many solutions are characterized by large values of  $\varepsilon_\omega$  and  $\varepsilon_p$ ; large scatterings for both the pressure and vorticity distributions can also be seen easily in Figures 2 and 3.

4. The  $\varepsilon_\omega$  values are much greater than the  $\varepsilon_p$ ; this is obvious because very large relative errors for  $\omega$  are probable near the separation and the reattachment points if the length and the position of the separation region are not computed very accurately. Also, most of the computations use the

Table II. Wall vorticity values for  $Re = 10$ 

$x/x_{out}$	WA2	A	DG	G	GBV	GF	H	K	LD	MN	PSW	QN	R	S	WAI	CJG
0.00	3.0000	—	2.9890	2.9900	2.9700	2.9710	3.0000	3.0000	3.0000	3.0113	3.0000	3.0750	3.0000	3.0000	3.0000	3.0000
0.05	2.5660	—	2.9320	2.5600	2.3000	2.2170	2.5760	2.5800	2.4000	2.5809	2.6100	2.5415	2.4000	2.5812	1.6710	2.5750
0.10	1.8200	—	1.8670	1.8240	1.6300	1.4470	1.6977	1.7000	1.7200	1.6524	1.6980	1.7594	1.4660	1.7002	0.9630	1.7060
0.15	0.9330	—	0.4577	0.6810	0.3300	0.2710	0.3923	0.7000	0.2400	0.4952	0.3920	0.4004	0.0600	0.3982	0.1870	0.3990
0.20	0.1520	—	-0.0435	0.0540	-0.0300	-0.2330	-0.0924	0.0300	-0.0800	-0.0842	-0.0920	-0.1201	-0.0800	-0.0961	-0.0570	-0.1000
0.25	0.0160	—	-0.0851	-0.0790	-0.1000	-0.2280	-0.1311	-0.1000	-0.1300	-0.1302	-0.1300	-0.1312	-0.1000	-0.1329	-0.0930	-0.1350
0.30	-0.0510	—	-0.1042	-0.0760	-0.1000	-0.1670	-0.1074	-0.1000	-0.0900	-0.1091	-0.1250	-0.1075	-0.1220	-0.1071	-0.0850	-0.1080
0.35	-0.0002	—	-0.0996	-0.0690	-0.0800	-0.1470	-0.1043	-0.0900	-0.1100	-0.1035	-0.1180	-0.1044	-0.1240	-0.1050	-0.0810	-0.1060
0.40	0.0450	—	-0.0874	-0.0570	-0.0700	-0.1420	-0.1015	-0.0700	-0.1200	-0.0995	-0.1020	-0.1034	-0.1040	-0.1030	-0.0770	-0.1030
0.45	0.0640	—	-0.0536	-0.0280	-0.0300	-0.1220	-0.0772	-0.0400	-0.0900	-0.0733	-0.0800	-0.0792	-0.0620	-0.0787	-0.0710	-0.0790
0.50	0.0900	—	-0.0010	0.0190	0.0000	-0.0810	-0.0293	0.0200	-0.0300	-0.0261	-0.0350	-0.0327	0.0000	-0.0320	-0.0520	-0.0330
0.55	0.1330	—	0.0614	0.0760	0.0700	-0.0230	0.0327	0.0700	0.0200	0.0338	0.0250	0.0276	0.0660	0.0283	-0.0270	0.0270
0.60	0.1830	—	0.1261	0.1380	0.1300	0.0420	0.1009	0.1300	0.0900	0.0989	0.0840	0.0936	0.1320	0.0938	0.0090	0.0920
0.65	0.2360	—	0.1884	0.2010	0.2000	0.1090	0.1705	0.1900	0.1500	0.1629	0.1480	0.1593	0.2000	0.1591	0.0460	0.1570
0.70	0.2900	—	0.2451	0.2620	0.2700	0.1730	0.2384	0.2500	0.2200	0.2225	0.2040	0.2209	0.2320	0.2207	0.0810	0.2170
0.75	0.3450	—	0.2939	0.3210	0.3000	0.2330	0.3034	0.3000	0.2600	0.2761	0.2560	0.2766	0.2660	0.2765	0.1130	0.2720
0.80	0.4050	—	0.3331	0.3770	0.3500	0.2840	0.3652	0.3400	0.3100	0.3228	0.2960	0.3257	0.3000	0.3251	0.1270	0.3190
0.85	0.4740	—	0.3611	0.4280	0.3500	0.3270	0.4230	0.3900	0.3400	0.3614	0.3300	0.3667	0.3320	0.3652	0.1650	0.3570
0.90	0.5590	—	0.3766	0.4730	0.3300	0.3590	0.4753	0.4300	0.3400	0.3869	0.3400	0.3943	0.3320	0.3957	0.1780	0.3850
0.95	0.6610	—	0.3811	0.5070	0.3200	0.3790	0.5152	0.4500	0.3400	0.4108	0.3660	0.4122	0.3320	0.4151	0.1920	0.4020
1.00	0.7530	—	0.3856	0.5210	0.3100	0.3840	0.5317	0.4700	0.3400	0.4341	0.3926	0.4215	0.3320	0.4220	0.1970	0.4080

Table III. Wall vorticity values for  $Re = 100$

$x/x_{out}$	WA2	A	DG	G	GBV	GF	H	K	LD	MN	PSW	QN	R	S	WA1	CIG
0.00	3.0000	—	2.9890	2.9260	3.0000	2.9720	3.0000	3.0000	3.0000	2.9969	3.0000	2.9983	3.0000	3.0000	3.0000	3.0000
0.05	2.3730	—	2.5510	2.5000	2.5000	2.4690	2.5109	2.4900	2.5300	2.4837	2.6020	2.4727	2.5000	2.5024	1.8170	2.5016
0.10	1.6770	—	1.8270	1.7720	1.7700	1.6940	1.7082	1.7300	1.7400	1.6934	1.8500	1.6904	1.8600	1.7217	1.2660	1.7216
0.15	1.0490	—	0.8476	0.8290	0.7400	0.7790	0.7284	0.8100	0.7400	0.7544	0.9000	0.7311	1.0000	0.7312	0.5490	0.7315
0.20	0.3810	—	0.1156	0.1990	0.2500	0.1440	0.1116	0.1200	0.1000	0.1069	0.1300	0.0910	0.3320	0.1019	0.0880	0.1018
0.25	0.2720	—	-0.1505	-0.0170	-0.0300	-0.0810	-0.0898	-0.0700	0.0600	-0.0838	-0.1350	-0.0863	-0.1320	-0.0957	-0.0620	-0.0954
0.30	0.1960	—	-0.1858	-0.0600	-0.1500	-0.1180	-0.1237	-0.1300	0.1200	-0.1231	-0.1880	-0.1208	-0.2000	-0.1274	-0.0960	-0.1280
0.35	0.1550	—	-0.1377	-0.0370	-0.1000	-0.0890	-0.0936	-0.1000	0.1000	-0.0951	-0.1450	-0.0928	-0.1320	-0.0968	-0.0810	-0.0981
0.40	0.1230	—	-0.0482	0.0220	-0.0300	-0.0310	-0.0273	-0.0400	-0.0300	-0.0330	-0.0650	-0.0294	-0.0600	-0.0313	-0.0390	-0.0320
0.45	0.2770	—	-0.0551	0.0980	0.0800	0.0520	0.0568	0.0500	-0.0600	0.0536	0.0400	0.0561	0.0600	0.0525	0.0160	0.0513
0.50	0.3420	—	0.1539	0.1770	0.1700	0.1350	0.1449	0.1500	0.1400	0.1377	0.1400	0.1424	0.2000	0.1392	0.0760	0.1386
0.55	0.4000	—	0.2413	0.2520	0.2700	0.2240	0.2285	0.2300	0.2200	0.2242	0.2280	0.2277	0.0266	0.2226	0.1330	0.2220
0.60	0.4510	—	0.3164	0.3200	0.3500	0.2950	0.3043	0.3000	0.3000	0.2948	0.3000	0.3012	0.4000	0.2981	0.1860	0.2973
0.65	0.4870	—	0.3806	0.3810	0.4200	0.3680	0.3713	0.3700	0.3600	0.3646	0.3720	0.3697	0.4660	0.3646	0.2330	0.3638
0.70	0.5420	—	0.4354	0.4330	0.4800	0.4210	0.4296	0.4200	0.4200	0.4186	0.4240	0.4245	0.6000	0.4229	0.2730	0.4223
0.75	0.5790	—	0.4823	0.4790	0.5300	0.4790	0.4799	0.4600	0.4800	0.4694	0.4720	0.4759	0.6400	0.4730	0.3080	0.4729
0.80	0.6140	—	0.5225	0.5180	0.5700	0.5140	0.5232	0.5000	0.5200	0.5150	0.5080	0.5229	0.5000	0.5161	0.3390	0.5156
0.85	0.6440	—	0.5570	0.5520	0.6200	0.5590	0.5599	0.5300	0.5600	0.5454	0.5480	0.5583	0.4660	0.5530	0.3660	0.5524
0.90	0.6720	—	0.5871	0.5810	0.6300	0.5800	0.5910	0.5600	0.6000	0.5820	0.5800	0.5780	0.5200	0.5844	0.3900	0.5843
0.95	0.7000	—	0.6152	0.6060	0.6500	0.6160	0.6162	0.5700	0.6270	0.6179	0.6200	0.5984	0.5340	0.6103	0.4090	0.6101
1.00	0.7250	—	0.6433	0.6280	0.6700	0.6160	0.6378	0.5800	0.6270	0.6530	0.6600	0.6206	0.5600	0.6228	0.4210	0.6210

Table IV. Wall pressure values for  $Re = 10$

$x/x_{out}$	WA2	A	DG	G	GBV	GF	H	K	LD	MN	PSW	QN	R	S	WAI	CJG
0.00	-0.0450	-0.2890	-0.2094	-0.2690	-0.3125	-0.4460	-0.4154	-0.2300	-0.3240	-0.3088	-0.3028	--	-0.1625	--	-0.0830	-0.6650
0.05	-0.0500	-0.2840	-0.2523	-0.3040	-0.2900	-0.3880	-0.3187	-0.2400	-0.3140	-0.3163	-0.3166	--	-0.1450	--	-0.1020	-0.3170
0.10	-0.0640	-0.2610	-0.2952	-0.3200	-0.2675	-0.3370	-0.3386	-0.2400	-0.3100	-0.3113	-0.3280	--	-0.1250	--	-0.1060	-0.3400
0.15	-0.0480	-0.2160	-0.2339	-0.2570	-0.2150	-0.2610	-0.2602	-0.2050	-0.2400	-0.2467	-0.2620	--	-0.0750	--	-0.0810	-0.2620
0.20	-0.0350	-0.1560	-0.1458	-0.1520	-0.1400	-0.1640	-0.1497	-0.1400	-0.1560	-0.1514	-0.1660	--	-0.0375	--	-0.0570	-0.1510
0.25	-0.0200	-0.1040	-0.1001	-0.0960	-0.0875	-0.1020	-0.0933	-0.0960	-0.0940	-0.0948	-0.1063	--	-0.0225	--	-0.0400	-0.0920
0.30	-0.0090	-0.0710	-0.0756	-0.0700	-0.0600	-0.0740	-0.0683	-0.0700	-0.0680	-0.0680	-0.0781	--	-0.0175	--	-0.0290	-0.0680
0.35	-0.0080	-0.0520	-0.0553	-0.0530	-0.0450	-0.0560	-0.0529	-0.0500	-0.0500	-0.0514	-0.0556	--	-0.0125	--	-0.0190	-0.0530
0.40	-0.0060	-0.0350	-0.0362	-0.0360	-0.0300	-0.0390	-0.0358	-0.0320	-0.0320	-0.0351	-0.0370	--	-0.0100	--	-0.0110	-0.0370
0.45	-0.0030	-0.0180	-0.0174	-0.0180	-0.0150	-0.0190	-0.0178	-0.0170	-0.0160	-0.0173	-0.0196	--	-0.0050	--	-0.0070	-0.0180
0.50	0.0000	0.0000	0.0000	0.0000	0.0000	0.0000	0.0000	0.0000	0.0000	0.0000	0.0000	--	0.0000	--	0.0000	0.0000
0.55	0.0040	0.0170	0.0151	0.0160	0.0175	0.0180	0.0165	0.0170	0.0160	0.0156	0.0149	--	0.0075	--	0.0060	0.0160
0.60	0.0070	0.0320	0.0278	0.0300	0.0275	0.0330	0.0302	0.0300	0.0280	0.0289	0.0284	--	0.0125	--	0.0130	0.0300
0.65	0.0100	0.0440	0.0380	0.0410	0.0375	0.0460	0.0413	0.0420	0.0400	0.0397	0.0392	--	0.0200	--	0.0190	0.0410
0.70	0.0170	0.0550	0.0459	0.0500	0.0425	0.0570	0.0504	0.0500	0.0480	0.0482	0.0482	--	0.0220	--	0.0230	0.0500
0.75	0.0180	0.0640	0.0520	0.0570	0.0500	0.0650	0.0574	0.0600	0.0560	0.0548	0.0560	--	0.0270	--	0.0270	0.0570
0.80	0.0160	0.0710	0.0565	0.0610	0.0550	0.0710	0.0613	0.0650	0.0640	0.0598	0.0605	--	0.0310	--	0.0300	0.0620
0.85	0.0160	0.0760	0.0599	0.0640	0.0600	0.0660	0.0636	0.0700	0.0680	0.0633	0.0656	--	0.0330	--	0.0330	0.0660
0.90	0.0140	0.0810	0.0628	0.0630	0.0675	0.0790	0.0634	0.0720	0.0720	0.0654	0.0692	--	0.0350	--	0.0350	0.0680
0.95	0.0080	0.0850	0.0660	0.0610	0.0725	0.0810	0.0603	0.0720	0.0740	0.0673	0.0734	--	0.0370	--	0.0370	0.0700
1.00	-0.0030	0.0860	0.0691	0.0590	0.0775	0.0830	0.0560	0.0720	0.0760	0.0692	0.0797	--	0.0380	--	0.0380	0.0710

Table V. Wall pressure values for  $Re = 100$

$x/x_{out}$	WA2	A	DG	G	GBV	GF	H	K	LD	MN	PSW	QN	R	S	WAI	CJG
0.00	-0.0010	-0.2120	-0.2239	-0.2220	-0.2400	-0.2200	-0.2114	-0.2100	-0.2175	-0.2312	-0.1940	-	-0.1050	-	-0.0650	-0.2147
0.05	-0.0060	-0.2220	-0.2288	-0.2340	-0.2225	-0.2280	-0.2359	-0.2200	-0.2335	-0.2299	-0.2240	-	-0.1050	-	-0.0770	-0.2357
0.10	-0.0110	-0.2210	-0.2337	-0.2260	-0.2050	-0.2180	-0.2281	-0.2200	-0.1775	-0.2204	-0.2320	-	-0.1000	-	-0.0730	-0.2275
0.15	-0.0150	-0.1890	-0.2052	-0.1830	-0.1650	-0.1800	-0.1848	-0.1800	-0.1895	-0.1809	-0.2020	-	-0.0925	-	-0.0600	-0.1836
0.20	-0.0130	-0.1470	-0.1575	-0.1340	-0.1300	-0.1350	-0.1342	-0.1400	-0.1375	-0.1330	-0.1560	-	-0.0725	-	-0.0460	-0.1339
0.25	-0.0100	-0.1100	-0.1138	-0.0980	-0.0975	-0.0990	-0.0985	-0.1100	-0.1015	-0.0976	-0.1150	-	-0.0500	-	-0.0340	-0.0979
0.30	-0.0070	-0.0820	-0.0806	-0.0720	-0.0675	-0.0720	-0.0723	-0.0800	-0.0735	-0.0712	-0.0810	-	-0.0375	-	-0.0250	-0.0717
0.35	-0.0050	-0.0570	-0.0541	-0.0500	-0.0425	-0.0490	-0.0500	-0.0600	-0.0535	-0.0490	-0.0560	-	-0.0250	-	-0.0170	-0.0494
0.40	-0.0030	-0.0350	-0.0320	-0.0300	-0.0275	-0.0300	-0.0304	-0.0400	-0.0335	-0.0296	-0.0340	-	-0.0150	-	-0.0110	-0.0304
0.45	-0.0020	-0.0150	-0.0140	-0.0140	-0.0125	-0.0140	-0.0137	-0.0200	-0.0155	-0.0184	-0.0150	-	-0.0075	-	-0.0050	-0.0135
0.50	0.0000	0.0000	0.0000	0.0000	0.0000	0.0000	0.0000	0.0000	0.0000	0.0000	0.0000	-	0.0000	-	0.0000	0.0000
0.55	0.0010	0.0120	0.0106	0.0110	0.0100	0.0100	0.0108	0.0070	0.0105	0.0106	0.0100	-	0.0030	-	0.0050	0.0105
0.60	0.0020	0.0210	0.0183	0.0190	0.0175	0.0180	0.0190	0.0130	0.0185	0.0185	0.0180	-	0.0075	-	0.0080	0.0185
0.65	0.0020	0.0270	0.0237	0.0240	0.0200	0.0240	0.0249	0.0200	0.0225	0.0241	0.0240	-	0.0100	-	0.0100	0.0245
0.70	0.0020	0.0310	0.0271	0.0280	0.0225	0.0280	0.0288	0.0250	0.0225	0.0278	0.0280	-	0.0100	-	0.0120	0.0287
0.75	0.0030	0.0330	0.0290	0.0300	0.0250	0.0300	0.0311	0.0230	0.0225	0.0299	0.0300	-	0.0050	-	0.0130	0.0303
0.80	0.0030	0.0340	0.0296	0.0310	0.0200	0.0310	0.0320	0.0220	0.0225	0.0308	0.0300	-	0.0025	-	0.0140	0.0313
0.85	0.0040	0.0340	0.0292	0.0310	0.0175	0.0300	0.0317	0.0200	0.0225	0.0305	0.0300	-	0.0050	-	0.0150	0.0313
0.90	0.0040	0.0320	0.0278	0.0290	0.0150	0.0280	0.0305	0.0200	0.0225	0.0290	0.0300	-	0.0075	-	0.0150	0.0294
0.95	0.0030	0.0300	0.0255	0.0270	0.0125	0.0250	0.0285	0.0190	0.0225	0.0275	0.0260	-	0.0100	-	0.0140	0.0273
1.00	0.0030	0.0290	0.0231	0.0260	0.0100	0.0250	0.0258	0.0180	0.0225	0.0260	0.0220	-	0.0100	-	0.0140	0.0253

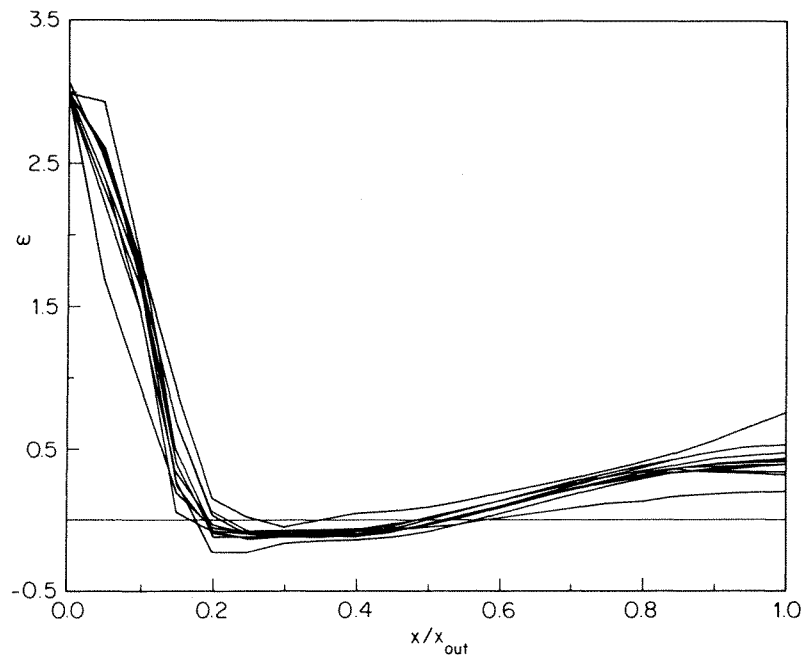
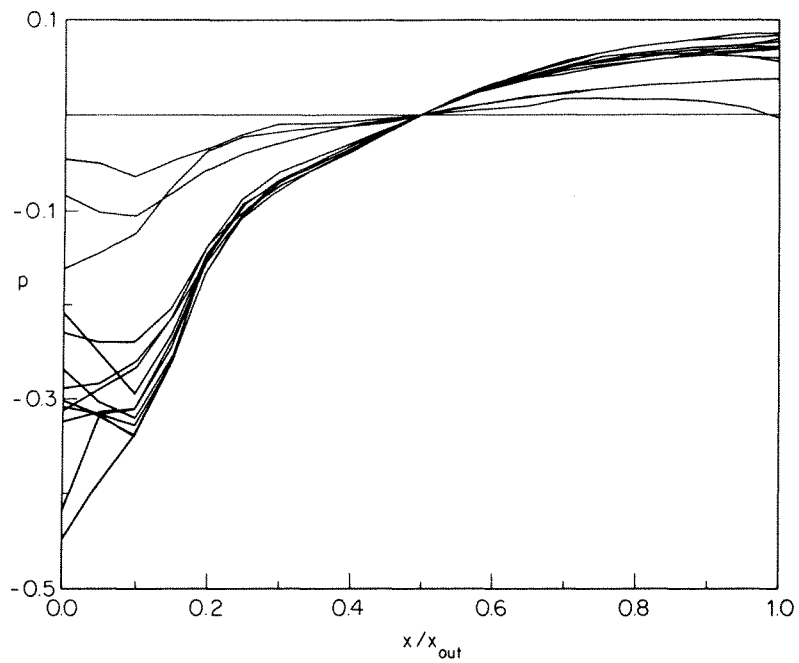
Figure 2. Vorticity distributions at the wall for  $Re = 10$ Figure 3. Pressure distributions at the wall for  $Re = 10$

Table VI. Summary of the results

CONTRIBUTOR	Problem 1 ( $Re = 10$ )				Problem 2 ( $Re = 100$ )					
	CPU	$\omega_{min}$	$\omega_{out}$	$\epsilon_{\omega}$	$\epsilon_p$	CPU	$\omega_{min}$	$\omega_{out}$	$\epsilon_{\omega}$	$\epsilon_p$
A	168.0	—	—	—	10.67	210.0	—	—	—	10.02
DG	9.6	-0.1042	0.3856	26.51	8.11	8.1	-0.1858	0.6433	14.64	6.77
G	5.9	-0.0790	0.5210	52.12	2.63	6.5	-0.0600	0.6280	33.06	1.43
GBV	120.8	-0.1000	0.3100	34.92	11.15	241.5	-0.1500	0.6700	23.15	17.61
GF	60.0	-0.2330	0.3840	48.98	10.72	280.0	-0.1180	0.6160	5.14	2.71
H	7.65	-0.1311	0.5317	9.22	2.24	7.65	-0.1237	0.6378	3.70	1.50
K	62.0	-0.1000	0.4700	41.21	8.24	146.0	-0.1300	0.5800	6.46	21.57
LD	6415.0	-0.1300	0.3400	10.75	4.81	2661.0	-0.0600	0.6270	42.13	12.31
MN	1.2	-0.1302	0.4341	6.70	3.44	1.4	-0.1231	0.6530	2.33	3.45
PSW	10.0	-0.1300	0.3928	6.30	4.97	8.13	-0.1880	0.6600	17.67	7.15
QN	104.0	-0.1312	0.4215	2.63	—	—	-0.1208	0.6206	3.50	—
R	19.0	-0.1240	0.3320	30.14	61.25	22.5	-0.2000	0.5600	43.11	61.16
S	168.0	-0.1329	0.4220	1.74	—	177.0	-0.1274	0.6228	0.44	—
WA2	3.91	-0.0510	0.7530	111.92	78.92	4.11	+0.1230	0.7250	135.48	90.43
WAI	—	-0.0930	0.1970	55.04	58.56	—	-0.0960	0.4210	32.83	59.98
CJG (benchmark)	—	-0.1350	0.4080	0.0	0.0	—	-0.1280	0.6210	0.0	0.0

primitive variables, so that the values of the vorticity at the wall are not necessarily a direct indication of the accuracy of the solution method.

5. Nothing definite can be said about the superior accuracy of finite elements or finite differences. In particular, two groups (MN and QN) have obtained solutions using the same variables on the same mesh but different discretization (FD and FE, respectively) obtaining comparable accuracy.

6. The mesh distribution employed in the calculations appears to be very important to model the separation region correctly. For example, the FD and FE solutions of MN and QN, using a proper stretching in the direction normal to the wall, are both satisfactory in spite of the overall coarseness of the mesh. A knowledge of the grid distributions used by the various participant groups could thus explain many of the discrepancies observed in the various solutions.

7. The CPU times required by the various methods vary significantly and certainly more than one could have anticipated. Besides the obvious differences among the numerical techniques employed by the participants (e.g. steady state vs. time dependent formulations), an important reason for such a result is believed to be that some of the solutions have been obtained by means of general purpose industrial packages, whereas others by 'academic codes' prepared just for the present problem.

8. For the case of a relatively simple geometry, no benefits are obtained using differential rather than algebraic or analytical co-ordinate transformations, in spite of the great difference in their computational costs. As a matter of fact, the CPU time required to generate the grid by solving a system of PDEs can be of the same order of that required to compute the flow field.

#### ACKNOWLEDGMENTS

The authors are grateful to all of the contributors for their co-operation and, in particular, to Prof. L. Quartapelle for many helpful suggestions and for a thorough revision of the manuscript. Prof. A. Di Carlo has provided considerable help to P. Orlandi in organizing the workshop. This work has been supported in part by the Ministero Pubblica Istruzione.

#### APPENDIX

B. J. Alfrink, Delft Hydraulics Laboratory, the Netherlands; presently at ENR Computer Services for Technology, Petten, the Netherlands.

ODYSSÉE is based on the use of curvilinear finite differences in space and of fractional steps in time. Convective and diffusive transports are solved separately.

The convective transports are treated by means of a third order explicit method of characteristics, which appears to be unconditionally stable.

The diffusive transports are treated implicitly. The resulting system of algebraic equations is solved by means of a standard successive over-relaxation (SOR) iterative scheme. Neumann-type boundary conditions are eliminated beforehand in order to aid convergence.

The solution of the Neumann problem for the pressure requires careful attention. Taking the pressure nodes staggered in space, the compatibility condition is satisfied exactly. As for the diffusive transports the elliptic operator yields again a nine point molecule. The solution of the resulting system of algebraic equations has now been obtained by means of Gaussian elimination with partial pivoting.

See Reference 4.

K. A. Cliffe, C. P. Jackson and A. C. Greenfield, AERE Harwell, U.K.

A finite element method is used to solve the Navier–Stokes equations in the primitive variables. The space  $W_h(\Omega)$  is generated by nine-node isoparametric elements with biquadratic interpolation. The space  $Q_h(\Omega)$  is generated by piecewise linear interpolation on the same elements; the interpolation is discontinuous across element boundaries. A Newton–Raphson linearization scheme is used, and the linear system is solved using the frontal solution method.

See Reference 3.

I. Demirovic and A. D. Gosman, Imperial College, London, U.K.

The method uses a semi-strong conservation form of the Navier–Stokes equations, written in terms of contravariant physical velocity components. The solution domain is overlaid by an arbitrary non-orthogonal mesh with quadrilateral curvilinear control volumes. The governing equations are discretized in the finite-volume fashion using hybrid differencing for the fluxes.

The presence of cross-derivatives pressure gradient and diffusion flux terms arising from the co-ordinate system non-orthogonality made the coefficient matrices nine-diagonal with the possibility of negative coefficients. The related problems have been solved to yield a stable solution procedure which operates in a manner similar to the SIMPLE algorithm, using iterative ADI to solve the simultaneous equations.

A report is in preparation.

J. Goussebaile, J. P. Benque and P. L. Viollet, Laboratoire National d'Hydraulique, Chatou, France.

To deal with general complex geometries non-orthogonal boundary fitted co-ordinates are used which allow an arbitrary choice of the co-ordinate lines. In fact we do not solve the equations in the real domain  $\Omega$  (with boundary  $\Gamma$ ) but we transform this physical domain, which is in the plane  $(x, y)$ , into a numerical domain  $\hat{\Omega}$ , in a plane  $(\xi, \eta)$  with a boundary  $\hat{\Gamma}$ , which is made only of vertical and horizontal lines. Then in the Navier–Stokes Boussinesq equations we transform the physical variables  $(x, y)$  into the computational variables  $(\xi, \eta)$  and solve the  $u, v, T$  equations in the transformed domain using a classical finite difference scheme. Although we could impose by hand point after point the discretized correspondence between  $\Omega$  and  $\hat{\Omega}$ , the use of some automatic process such as the Thompson method is preferred.

Using a first order approximation in time, we use a fractional step algorithm and compute auxiliary fields, the solutions of elementary problems: first convection, then diffusion, finally continuity, which are of different nature (hyperbolic, parabolic, elliptic). The convection is treated explicitly by a method of characteristics; the diffusion is treated fully implicitly. For each step, the initial values are given by the result of the previous step and the boundary conditions are estimated using the boundary conditions on the real fields  $u, v$  and  $T$ .

See References 5–7.

M. Grandotto, Commissariat a l'energie atomique, Cadarache B. P. N. 1, 13115 Saint Paul Lez Durance, France.

Method: standard Galerkin finite element method with penalization.

Elements:

1. Q1–Q0: 4 nodes, piecewise constant pressure, bilinear velocity
2. Q2–P1: 9 nodes, discontinuous linear pressure, biquadratic velocity.

Note: underparametric elements are used, i.e. straight sides and intermediate nodes located at the middle of sides.

Programm: NASTHY

Computer: CRAY-1.

See References 8 and 9.

G. Guj and B. Favini, Dipartimento di Meccanica ed Aeronautica, Università di Roma 'La Sapienza', Italy.

The solutions of the test problems 1 and 2 have been obtained using a computer code, named MAFEL3, which was developed in 1979 for the simulation of viscous laminar flows of an incompressible fluid in complex geometries. The Navier–Stokes equations are solved in terms of the primitive variables in the transformed computational domain using an extension of the MAC scheme (originally developed for rectangular grids) to curvilinear grids. Therefore the contravariant velocity components, located at cell midsides, are assumed as variables. The momentum equations are linearized updating the convective term, and the steady state solution is reached by means of an explicit time-integration technique. The artificial compressibility method of Chorin is used to obtain the pressure field from the continuity equation after every time-step. The spatial derivatives are discretized by standard second-order-accurate finite differences. The body-fitted curvilinear mesh is generated numerically solving a quasi-linear elliptic system in the transformed plane.

See Reference 10.

A. G. Hutton, Central Electricity Generating Board, Berkeley Nuclear Labs, Berkeley, Glos, U.K.

The Navier–Stokes equations were solved by the standard Galerkin finite element method with continuity incorporated by the method of Lagrange multipliers.

Two types of eight-noded, isoparametric, quadrilateral elements were used;

- (a) the well known serendipity quadratic velocity/linear pressure element (type 2)
- (b) boundary elements (type 3) distinguished from type 2 by the incorporation of the normal derivatives of velocity as additional nodal variables at the boundary nodes.

Type 3 elements were laid along the symmetry line and wall boundaries in such a way that element edges intersected these boundaries at right angles.

The outflow boundary conditions were  $v = 0$  and  $p - (\partial u / \partial x) / Re = 0$ .

The equation system was solved using Newton–Raphson iteration coupled with a direct frontal solver for the linear systems within each iteration.

The wall vorticity was evaluated at a node as  $\omega = \partial u \cos \theta - \partial v \sin \theta$ , where  $\theta$  is the angle between the wall normal at the node and the  $x$  co-ordinate direction and  $\partial u$ ,  $\partial v$  are the nodal values of the normal derivatives of the  $x$  and  $y$  velocity components (explicitly provided by the solution).

See Reference 11.

D. Khaletzky, NEYRPIIC, Grenoble, France.

A finite element method to solve the Navier–Stokes equations in primitive variables.

The method is time-marching with explicit advection and implicit diffusion. The explicit advection step uses the method of characteristics, with the aid of the shape functions of the elements. After determining  $u^*$  and  $v^*$  in this way, the Navier–Stokes equations read

$$\frac{\bar{v}^{n+1} - \bar{v}^*}{\delta t} = -\bar{\nabla} p^{n+1} + \nu \nabla^2 \bar{v}^{n+1}$$

Pressure is determined by solving the Poisson equation

$$\nabla^2 p^{n+1} = \frac{1}{\delta t} \bar{\nabla} \cdot \bar{v}^*$$

See Reference 12.

Latrobe, Delapierre, Centre d'études nucléaires de Grenoble, France.

The test problems have been solved by the computer code REYCUR, which is derived from WAPITI, presented at a previous IAHR meeting.

REYCUR, like WAPITI, uses a finite volume formulation, a semi-implicit type of discretization and solves at each time step a linear system for the pressure field. The two components of velocity are evaluated on a staggered grid after resolution of the Poisson-like pressure equation.

Another difference between REYCUR and WAPITI is related to the linear system solution method. In WAPITI, the matrix is factorized once and for all by the Cholesky method. This method is quite efficient and fast because, for incompressible flows, the matrix never has to be refactorized during the computed transient. But, although the matrix is banded and full advantage is taken of its structure, the computer storage needed by complete Cholesky factorization may be quite large. Consequently, REYCUR uses a partial Cholesky factorization coupled with a conjugate gradient iterative method.

The curvilinear co-ordinate system is generated by the code GENOR which enables us to generate such a system for arbitrary 2D geometries.

See References 13 and 14.

V. Magi and M. Napolitano, Istituto di Macchine, Università, di Bari, Italy.

The vorticity-stream-function Navier-Stokes equations are considered in a general curvilinear co-ordinate system, which maps an arbitrary two-dimensional domain in the physical plane into a rectangle in the computational plane. In the present applications an orthogonal mesh is generated by a simple algebraic method. The stream function equation is parabolized in time by means of a relaxation-like time derivative and the steady state solution is obtained by a time-marching two-sweep ADI method, which requires to solve only linear two-by-two block-tridiagonal systems. The difference equations are written in incremental form; windward differences are used for the incremental variables, for stability, whereas central differences approximate the non-incremental terms, for accuracy. In this way, at convergence, the solution is free of numerical viscosity and is second-order accurate.

See References 15 and 16.

L. Quartapelle, Istituto di Fisica, Politecnico di Milano, Italy.

M. Napolitano, Istituto di Macchine, Università di Bari, Italy.

The method solves the time dependent vorticity-stream-function Navier-Stokes equations by a split formulation. The vorticity equation is supplemented by its proper integral conditions and the transient solution is obtained by solving a cascade of elliptic problems (by means of the Cholesky decomposition method). The equations are discretized by a finite element method using bilinear quadrilateral elements.

The grid generated by Magi and Napolitano has been employed in conjunction with the standard isoparametric transformation technique.

See Reference 17.

J. D. Porter, J. Sykes and N. S. Wilkes, AERE Harwell, U.K.

An existing finite difference computer program for predicting turbulent flows in rectangular geometries has been generalized to complex geometries by means of the co-ordinate transformation method. The advantages of the method have previously been demonstrated by solving an equation for a scalar field convected around a cavity. In Reference 18 the procedure for solving the laminar flow equations is outlined and some results are given for a test problem.

A. K. Rasgoti, A. S. Veritas Research, Norway; presently at Universitat Karlsruhe, Germany.

Calculations for the test problems have been carried out by solving with finite differences the Navier–Stokes equations in orthogonal curvilinear co-ordinates. The orthogonal curvilinear co-ordinate system, i.e. the numerical grid, is generated by solving the Laplace equations for the physical co-ordinates by central differencing. Necessary details of this method can be seen in References 19 and 20. The momentum and continuity equations are then solved on the curvilinear numerical grid using control volume integration and hybrid differencing similar to that used in the TEACH code. The additional source terms appearing in the momentum equations as a result of the co-ordinate transformations were introduced after 60 iterations. Two hundred and fifty iterations were necessary to converge fluid flow solution for problems 1 and 2 and 300 iterations were required for the problem 3. Three hundred iterations were, however, performed for all the cases. Further details of the methods employed and their application can be seen in References 21 and 22.

W. Schonauer, Rechenzentrum der Universitat Karlsruhe, W. Germany.

Self-adaptive difference method, made available in the SLDGL general purpose program package. Transformation of the domain to a rectangular domain, which resulted in a non-orthogonal co-ordinate transformation:  $x$  remains,  $y \rightarrow \eta$  by  $y = y_1(x) + \eta(1 - y_1(x))$ . Solution in a velocity–vorticity formulation. Treatment of the mixed derivative in  $\omega$  by an auxiliary variable.

The results for  $Re = 10$  were computed on a self-adapted  $46 \times 32$  grid. It was not possible to get a result for  $Re = 100$  from that initial solution. So, we computed intermediate solutions with grid adaptation for  $Re = 20, 50$ . The final solution for  $Re = 100$  is computed on a  $41 \times 62$  grid. See Reference 23.

A. Wada, Central Research Institute of Electric Power Industry, Japan.

K. Adachi, Mitsubishi Research Institute, Japan.

A method by co-ordinate transformation using complex analytical functions was used. This method is composed of the following two steps:

1. Variable transformation.
  - (a) The object domain is mapped conformally into simple domains, such as a rectangular domain, by the use of complex analytical functions. Taking advantage of the fact that the real part and imaginary part of complex analytical functions are harmonic functions and conjugate with each other, these complex analytical functions can be obtained numerically.
  - (b) It is necessary to determine beforehand the differential equation system after co-ordinate transformation. In the Navier–Stokes equation system, no large variation of format takes place in the co-ordinate transformation by complex analytical functions, but as the differentiation of inverse functions of transformed functions appears, it is necessary to obtain beforehand the differentiation of inverse functions of complex analytical functions.
2. Difference method.

The differential equation system of the domain after variable transformation and thereon is put to difference calculation to carry out numerical computation. As the configuration of the object domain is simplified by variable transformation, handling of the boundary becomes easy. Moreover, as the format of the difference equation does not undergo a major change, owing to co-ordinate transformation, the existing high-precision difference equation against the Navier–Stokes equation can easily be applied.

## REFERENCES

1. R. M. Smith and A. G. Hutton, 'The numerical treatment of advection. A performance comparison of current methods', *Numerical Heat Transfer*, **5**, (4), 439–462 (1982).
2. P. Roache, 'Scaling of high Reynolds number weakly separated channel flows', *Symposium on Numerical and Physical Aspects of Aerodynamic Flows*, 1981.
3. K. A. Cliffe, C. P. Jackson and A. C. Greenfield, 'Finite element solutions for flow in a symmetric channel with a smooth expansion', *AERE-R. 10608*.
4. B. J. Alfrink, M. J. Officier, C. B. Vreugdenhil and H. G. Wind, 'Applications in hydraulics of a curvilinear finite difference method for the Navier–Stokes equations', *Proc. Int. Conf. Num. Meth. in Laminar and Turbulent Flow*, Seattle, 1983.
5. J. Goussebaile, 'Modelisation d'écoulements et de transferts de chaleur par une methode de differences finies en mailles curvilignes non orthogonales', *Rapport E.D.F.—D.E.R. He/41/81.27*.
6. P. Esposito, 'Resolution bidimensionelle des equations de transport par la methode des caracteristiques', *Rapport E.D.F.—E.D.R. He/41/81.16*.
7. P. L. Violette, J. P. Benque and J. Goussebaile, 'Two-dimensional numerical modelling of non isothermal flows for unsteady thermal-hydraulic analysis', *Rapport E.D.F.—D.E.R. He/44/82.10 et He/41/82.08*.
8. M. Bercovier and M. S. Engelman, *J. Comp. Physics*, **30**, 181–201 (1979).
9. M. S. Engelman, R. L. Sani, P. M. Gresho and M. Bercovier, *Int. j. numer. methods fluids* **2**, (1982).
10. A. Di Carlo, R. Piva and G. Guj, 'Computational schemes in general curvilinear coordinates for Navier–Stokes flows', *Notes on Numerical Fluid Mechanics*, **2**, Vieweg, Braunschweig, 1980, p. 36.
11. A. G. Hutton, 'Finite element boundary techniques for improved performance in computing Navier–Stokes and related heat transfer problems', *CEGB report RD/B/N4651/*; also in *Finite Elements in Fluids*, vol. IV, Wiley, 1979.
12. J. P. Hufferus and D. Khaletzky, 'A finite element method to solve the Navier–Stokes equations using the method of characteristics', *Int. j. numer. methods fluids*, **4**, 247–269 (1984).
13. R. Glowinski *et al.*, 'On an efficient new pre-conditioned conjugate gradient method', *Colloque I.N.R.I.A.*, Versailles, December 1979.
14. J. K. Dukowicz and J. D. Ramshaw, 'Tensor viscosity method for convection in numerical fluid dynamics', *J. Comp. Physics*, **32**, 71 (1979).
15. V. Magi and M. Napolitano, 'Calcolo del flusso laminare in un canale di geometria complessa', *VI congresso Nazionale AIMETA*, Genova, 7–9 October 1982.
16. M. Napolitano, 'Efficient ADI and spline ADI methods for the steady state Navier–Stokes equations', *Int. j. numer. methods fluids*, **4**, 1101–1115 (1984).
17. L. Quartapelle and M. Napolitano, 'A method for solving the factorized vorticity-stream function equations by finite elements', *Int. j. numer. methods fluids*, **4**, 109–125 (1984).
18. J. D. Porter, J. Sykes and N. S. Wilkes, 'Calculation of fluid flows using finite differences and the method of co-ordinate transformations I. Laminar flow through a smooth expansion using an orthogonal transformation', *AERE—R 10760*.
19. A. D. Gosman and R. J. R. Johns, 'A simple method for generating curvilinear orthogonal grids for numerical fluid mechanics calculations', *Mech. Eng. Dept. Imperial College, Report FS/79/23*, 1979.
20. S. B. Pope, 'The calculation of turbulent recirculating flows in general orthogonal coordinates', *J. Comp. Physics*, **26**, 1987 (1978).
21. A. K. Rastogi, 'Hydrodynamics and mass transport in pipelines perturbed by welded joint' *DNV Technical Report No. 82.0152*, 1982.
22. A. K. Rastogi, 'Hydrodynamics in tubes perturbed by curvilinear obstructions', to be published in *JFE*, 1984.
23. W. Schonauer, K. Raith and G. Glotz, 'The SLDGL-program package for the self-adaptive solution of nonlinear systems of elliptic and parabolic PDE's', in R. Vichnevetsky and R. S. Stephenman (eds), *Advances in Computer Methods for Partial Differential Equations*, **IV**, IMACS 1981, pp. 117–125.